Volume 59
Number 76
28 September 2023
Pages 11287–11444

ChemComm

Chemical Communications

rsc.li/chemcomm

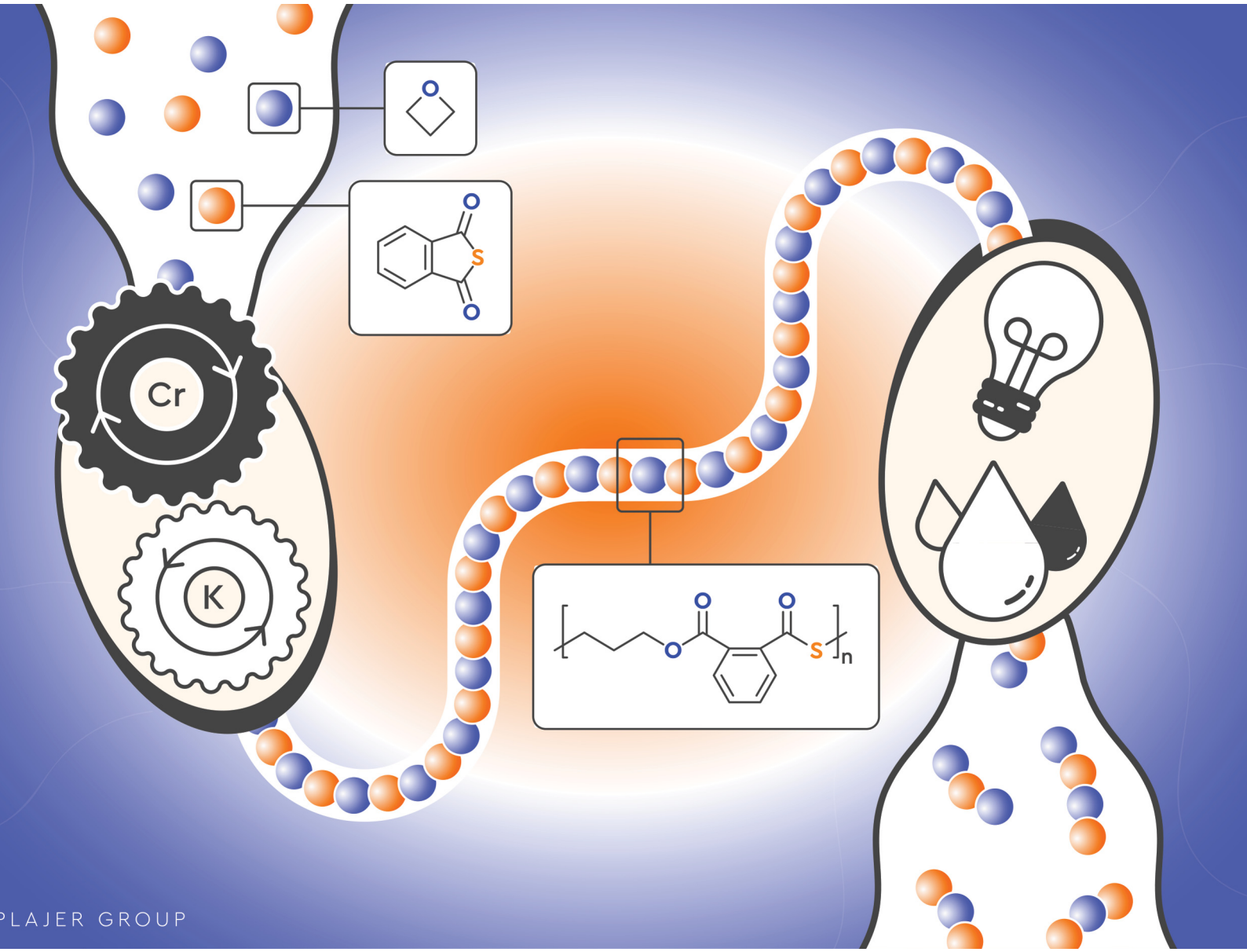

ISSN 1359-7345

ROYAL SOCIETY OF CHEMISTRY

COMMUNICATION

Alex J. Plajer *et al.*

Precise construction of weather-sensitive poly(ester-*alt*-thioesters) from phthalic thioanhydride and oxetane

ChemComm

COMMUNICATION

View Article Online
View Journal | View Issue

Cite this: *Chem. Commun.*, 2023, 59, 11353

Received 13th July 2023,
Accepted 22nd August 2023

DOI: 10.1039/d3cc03315e

rsc.li/chemcomm

Precise construction of weather-sensitive poly(ester-*alt*-thioesters) from phthalic thioanhydride and oxetane†

Christoph Fornacon-Wood, [a] Merlin R. Stühler,[a] Cesare Gallizioli,[a] Bhargav R. Manjunatha, [a] Volker Wachtendorf, [b] Bernhard Schartel [b] and Alex J. Plajer *[a]

We report the selective ring opening copolymerisation (ROCOP) of oxetane and phthalic thioanhydride by a heterobimetallic Cr(III)K catalyst precisely yielding semi-crystalline alternating poly(ester-*alt*-thioesters) which show improved degradability due to the thioester links in the polymer backbone.

Incorporating sulfur atoms into the polymer main chain rationally introduces unique material properties and functions compared to their all oxygen counterparts.[1–12] In particular sulfuration renders polymers more susceptible to photolysis and oxidation although investigations are usually limited to artificial conditions involving irradiation of polymer solution with intense UV light or exposure to excess chemical agents.[13–16] Sulfur containing polymers such as polythioesters are usually synthesized *via* polycondensation routes or ring-opening polymerisation (ROP), yet these methods only give access to a limited number of polymer structures.[17–19] Relatedly, ring-opening copolymerisation (ROCOP) of a strained heterocycle with heteroallenes is a popular method for the synthesis of heteroatom containing oxygenated polymers such as polycarbonates and polyesters which offers modular access to a wide range of polymer structures.[20–22] Sulfur analogous are also accessible such as polythiocarbonates from the ROCOP of CS_2 and polythioesters from the ROCOP of cylic thioanhydride (Fig. 1(a)).[14,15,23–28] Most relevant to our study are reports on phthalic thioanhydride (PTA)/epoxide ROCOP yielding semi-aromatic poly(thioester-*alt*-esters).[29–32] Although alternating ROCOP was achieved, transesterification side-reactions, particularly at higher reaction temperatures, were occasionally observed to reduce the sequence selectivity and related side-reactions can reduce the maximally achievable molecular weights.[20,33]

This notion helps to explain why maximum obtainable molecular weights were limited to 65 kg mol^{-1} ($Đ$ = 1.7). Relatedly, CS_2/epoxide ROCOP was likewise plagued with numerous side-reactions.[34]

Tackling this problem, we recently reported that a heterobimetallic Cr(III)K catalyst **LCrK** (Fig. 1(b)) enables the selective copolymerisation of CS_2 and oxetane (OX) to poly(trimethylene-dithiocarbonate) in 99% polymer and up to 96% linkage selectivity.[35] Unfortunately, the CS_2/OX copolymers show low thermal stability and start to decompose at *ca.* 160 °C and are highly susceptible to depolymerisation, to cyclic dithiocarbonates limiting their use in material applications. Nevertheless, the suppression of side-reactions demonstrates that heterobimetallic catalysis could be a promising tool for the synthesis of sulfurated ROCOP polymers. This prompted us to investigate the copolymerisation of OX with PTA employing **LCrK** which we report in this contribution.

Accordingly, we performed PTA/OX ROCOP with **LCrK** (Table 1) at a loading of 1 eq. **LCrK**: 1000 eq. PTA: 1000 eq. OX at 80 °C for 140 min producing a highly viscous mixture which solidified upon cooling. NMR analysis of the crude mixture reveals 99% PTA and OX consumption and a symmetric spectrum indicative of a highly regular polymer. 1D and 2D NMR as well as IR spectra conclusively show alternating esters ($\delta(C^q)$ = 166.5 ppm; $\tilde{\nu}$ = 1720 cm^{-1}) and thioesters ($\delta(C^q)$ = 194.6 ppm; $\tilde{\nu}$ = 1660 cm^{-1}) links making up the poly(ester-*alt*-thioester) (ESI,† Section S3). No extra signals can be observed in the ^{1}H or ^{13}C NMR spectrum leading us to conclude that no erroneous links from co-occurring side-processes other than alternating propagation are part of the polymer. This is further supported by the circumstance that the aromatic region of the ^{1}H NMR spectrum shows a profile equivalent to previous PTA copolymers that exhibit an alternate microstructure.[29–32] GPC analyses shows a bimodal molecular weight distribution with a M_n = 52.1 kg mol^{-1} ($Đ$ = 1.4) which is somewhat lower than the theoretical $M_{n,theo.}$ of 111.2 kDa assuming initiation from both OAc coligands of **LCrK**. MALDI-ToF mass spectrometry of a low M_n oligomer confirms the molecular formula corresponding to a

[a] *Institut für Chemie und Biochemie, Freie Universität Berlin, Fabeckstraße 34-36, Berlin 14195, Germany. E-mail: plajer@zedat.fu-berlin.de*
[b] *Bundesanstalt für Materialforschung und -Prüfung (BAM), Unter den Eichen 87, Berlin 12205, Germany*

† Electronic supplementary information (ESI) available. See DOI: https://doi.org/10.1039/d3cc03315e

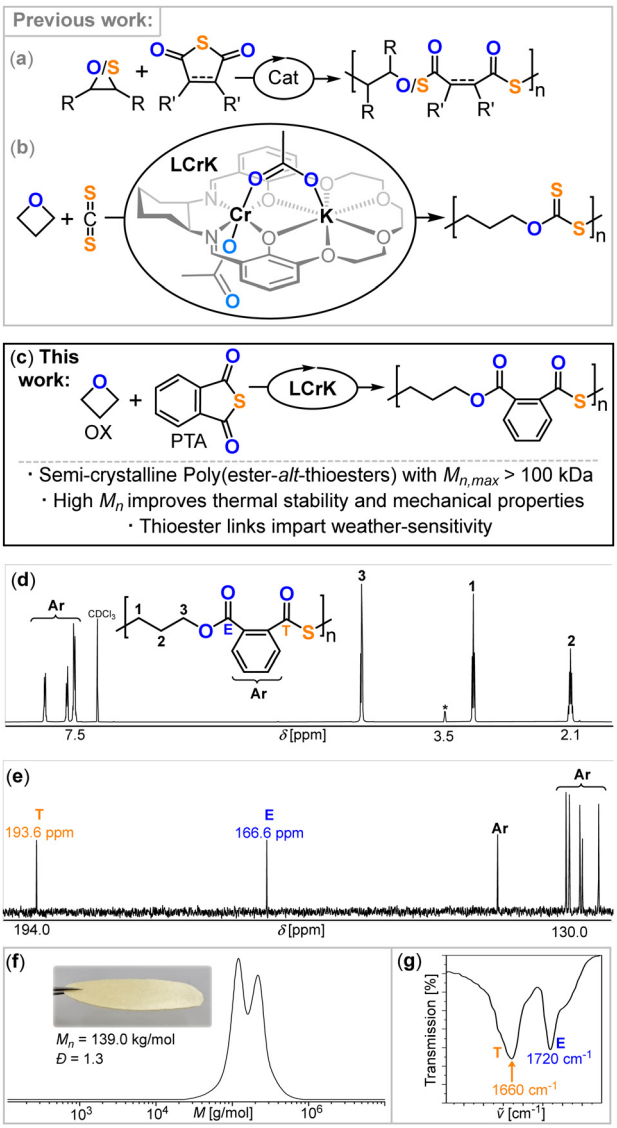

Fig. 1 (a) ROCOP of thioanhydrides with epoxides or thiiranes yielding polythioesters. (b) ROCOP of oxetane with CS_2 under **LCrK** catalysis. (c) ROCOP of oxetanes and thioanhydrides investigated in this report. (d) ^{1}H ($CDCl_3$, 400 MHz) and (e) zoom into the $^{13}C\{^1H\}$ NMR spectrum ($CDCl_3$, 126 MHz) of polymer obtained from Table 1 run #1. *Denotes residual MeOH from workup. (f) GPC trace with photograph of the hot-pressed material and (g) carbonyl region of the IR spectrum corresponding to Table 1 run #8.

one to one ester to thioester composition and reveals α-OAc, ω-OH functional chains (from OAc initiation and termination *via* chain-end protonation during work-up). Furthermore, the ^{31}P end-group test also confirms the formation of primary alcohol chain ends. However, chain-transfer processes with protic impurities as often observed in ROCOP cannot be ruled out to reduce molecular weights forming α,ω-OH functional chains which tentatively explain the bimodal molecular weight distribution.[20,36] Next, we surveyed the effect of catalyst choice employing the sodium derivative **LCrNa** and the rubidium derivative **LCrRb** and found these to be equally selective but less active than the potassium derivative in the order **LCrK** (TOF 435 h^{-1}) > **LCrRb** (TOF 275 h^{-1}) > **LCrNa**

Table 1 PTA/OX ROCOP with **LCrK**

Cat	Cat : OX : PTA	t [h]	Conv. [%][a]	M_n [kDa] ($Đ$)[b]
LCrK	1 : 10^3 : 10^3	2.3	99	52.1 (1.4)
LCrNa	1 : 10^3 : 10^3	5	56	17.1 (1.2)
LCrRb	1 : 10^3 : 10^3	2	55	23.8 (1.2)
L′Cr + KOAc@18c6	1 : 10^3 : 10^3	3	99	44.7 (1.5)
L′Cr	1 : 10^3 : 10^3	24	—	—
KOAc @18c6	1 : 10^3 : 10^3	24	—	—
LCrK	1 : 2 × 10^3 : 2 × 10^3	7	77	65.8 (1.2)
LCrK	1 : 4 × 10^3 : 4 × 10^3	24	88	139.0 (1.3)

Quantitative polymer selectivity is observed in all cases. [a] Relative integral in the normalised ^{1}H NMR spectrum of aromatic resonances from residual PTA *versus* polymer. [b] Determined by GPC (gel permeation chromatography) measurements conducted in THF, using narrow polystyrene standards to calibrate the instrument.

(TOF 112 h^{-1}). To mimic the electronic and coordinative situation in **LCrK** albeit as distinct components, we then employed a bicomponent catalyst comprising a bis-methoxy substituted $(MeO)_2$-SalCyCrOAc complex **L′Cr** (see ESI,† Section 2 for the structure) with KOAc@18-crown-6. This combination likewise showed excellent selectivity and activity. In contrast **L′Cr** or KOAc@18-crown-6 by themselves show no appreciable activity. Taken together our results indicate that ensuring heterobimetallic cooperativity employing Cr and K in combination rather than fixing both metals within the same scaffold is needed to achieve PTA/OX ROCOP. Having identified **LCrK** as a potent catalyst we decreased the catalyst loading to obtain higher molecular weight materials and indeed obtained an M_n of 65.8 kg mol^{-1} ($Đ$ = 1.2) from a run at 1 **LCrK:** 2000 PTA: 2000 OX and a maximum M_n of 139.0 kg mol^{-1} ($Đ$ = 1.3) from a run at 1 **LCrK:** 4000 PTA: 4000 OX. Note this $M_{n,max}$ represents a more than two-fold improvement over ROCOP thioesters, while even for ROCOP in general few examples exist with M_n's exceeding 100 kg mol^{-1}.[20,28–32] The materials are in all cases obtained as brittle powdery solids after precipitation. Differential scanning calorimetry reveals a melting point at T_m = 88.3 °C in the first heating cycle, yet no crystallisation in the following heating/cooling cycles is observed indicating slow crystallization; glass transition occurs at T_g = 23.2 °C (Fig. 2(a)). Previously semi-crystalline poly(thioester-*alt*-esters) from PTA could only be generated *via* stereocomplexation of variants derived from enantiopure epoxides.[32]

Thermogravimetric analysis reveals an increase in thermal stability with increasing M_n from $T_{d,5\%}$ *ca.* 285 °C (M_n = 17.1 and 52.1 kg mol^{-1}) to *ca.* 330 °C (M_n = 139.0 kg mol^{-1}) (Fig. 2(b)). This improvement is more pronounced when considering the onset of thermal degradation revealing some decomposition to already occur at 150 °C for the lower M_n samples while no decomposition occurs until 300 °C for the highest M_n copolymer. In comparison, the related propylene oxide copolymers of PTA exhibit a thermal decomposition onset at *ca.* 200 °C revealing an improvement of *ca.* 100 °C compared to our PTA/OX copolymers which is enabled by the increase in $M_{n,max.}$ compared to those.[29,31] In terms of other material properties, uniaxial tensile testing of copolymer films reveals an increase in ultimate strength with molecular weight from σ_b = 2.4 MPa for 17.1 kg mol^{-1} to σ_y = 8.3 MPa (ε_y = 5% strain)

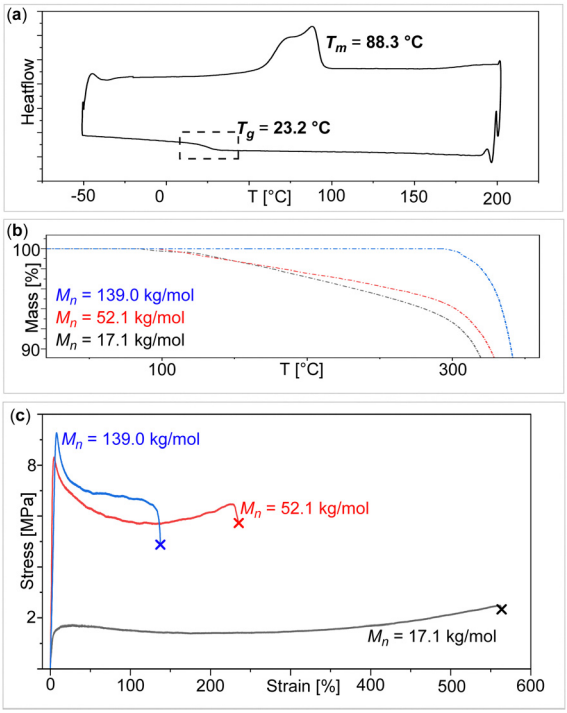

Fig. 2 (a) DSC curve (first heating and second cooling cycle) of copolymer corresponding to Table 1 run #8. (b) TGA and (c) tensile stress–strain curves of copolymers at different molecular weights.

for 52.1 kg mol^{-1} to σ_y = 9.3 MPa (ε_y = 8% strain) for 139.0 kg mol^{-1} (Fig. 2(c)). Furthermore, the samples become somewhat more brittle with increasing molecular weight showing decreasing ε_b at 560%, 234% and 137% strain respectively. For comparison, commodity LDPE exhibits a σ_b = 12 MPa at ε_b = 385% strain.[37] We infer that the increase in strength in the higher M_n samples is a consequence of higher degrees of crystallinity which is also apparent from the increasing opaqueness of the highest M_n film. The latter could be also tentatively confirmed by WAXS revealing more features in the higher M_n samples although the broad nature of these prevents quantification of the crystallinity.

Previously, sulfur containing links lead to oxidative and photodegradability benefits due to the lability of the C–S bond.[13–15] Accordingly, we suspended the high M_n PTA/OX copolymer (Table 1 run #8) in aqueous H_2O_2 for 1 week and observed complete degradation with no insoluble products remaining. ^{1}H NMR in D_2O reveals desymmetrisation of the initially highly symmetric starting spectrum due to the oxidative cleavage producing short chain oligomers. Likewise broadband UV irradiation of a $CDCl_3$ solution of the copolymer for 1 week led to degradation into oligomers with M_n < 2.5 kDa; related all-ester ROCOP polymers remain intact under these conditions.[15] As photooxidation and -degradation represent some of the primary breakdown pathways of polymer waste in nature prior to biodegradation we hypothesized that the thioester links could also enhance the degradability of our materials in a scenario closer to what happens with uncollected waste in the environment.[38] Note that although management plans exist, approximately 22% of plastic is leaking into the environment as uncollected litter after use.[39] Therefore degradability due to natural weathering factors (UV, heat, humidity, rain) was investigated using artificial weathering, employing films of the PTA/OX copolymers (see ESI,† Section S4). The scenario being that the respective material was exposed outdoors to natural weathering lying on the ground. A cycle that incorporated UV, rain and dry phases and changing temperatures with a maximum of 30 °C was applied (adapted from ISO standard 4892-3 : 2016). The equivalent of the 336 hours artificial weathering resulting in an UV radiant exposure of 54 MJ m^{-2} is about 4 months of natural weathering in Central Europe based on the UV radiative exposure. Note that lamps, that don't show spectral contributions below the solar cut-off around 290 nm were employed to ensure comparability with irradiation by sunlight. Weathering led to a brown discolouration (Fig. 3(a)) as well as increasing brittleness which caused cracking of some of the polymer films, the latter being potentially beneficial for the mechanical breakdown of the material in a real-world scenario. GPC analysis of the film (Table 1 run #8, M_n = 139.0, $Đ$ = 1.3) after weathering shows a decrease in molecular weight down to M_n *ca.* 9 kDa (Fig. 3(c)) and a significant broadening of the weight distribution to $Đ$ = 5.8 and together with the increase in brittleness, this could

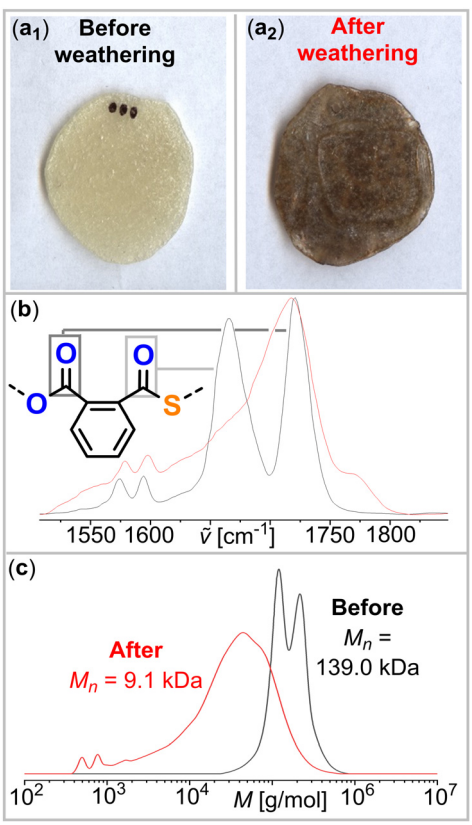

Fig. 3 Photographs of PTA/OX film (from copolymer of Table 1 run #8) (a_1) before and (a_2) after weathering. (b) Zoom into the C=O region of the surface ATR-IR spectrum. (c) GPC trace of material before and after weathering.

indicated some co-occurring photo crosslinking of chains alongside degradation. Nevertheless, the samples remain soluble in organic solvents such as THF after weathering. The surface IR spectra (Fig. 3(b)) reveal thioester groups ($\tilde{\nu}$ = 1660 cm^{-1}) on the film surface are more affected by weathering than the ester groups ($\tilde{\nu}$ = 1720 cm^{-1}). Accordingly control samples of commercial semi-aromatic polyesters (PET and PBT) show negligible weathering under identical conditions clearly highlighting the degradability benefits thioester links introduce. However, this circumstance might also limit the utility of these materials in a real-world scenario due to reduced durability of some consumer products.

In conclusion, we have developed a new synthetic methodology to yield semi-crystalline poly(ester-*alt*-thioesters) from the copolymerisation of phthalic thioanhydride and oxetane under heterobimetallic Cr(III)K catalysis. Hereby we obtain a high maximum M_n of 139.0 kg mol^{-1} corresponding to improved thermal stability compared to lower molecular weight and related literature known polymers. Metal choice and cooperativity are key to maximize catalytic performance, as individually Cr(III) and K complexes do not produce copolymer. Furthermore, moving from the lower to the higher end M_n materials reported in this study results in an approximate fourfold increase in maximum strength. Lastly, we found that the PTA/OX copolymers clearly benefit from the lability of the thioester bonds in terms of degradability under laboratory and environmental weathering conditions. Therefore, polythioesters could potentially be considered more sustainable materials than their all-oxygen counterparts which continue to contribute to plastic pollution.

The VCI is acknowledged for a Liebig Fellowship for A. J. P. and a PhD scholarship for C. G. Prof. Dr Christian Müller and Prof. Dr Rainer Haag are thanked for continuous support and valuable discussions. Glen J. Smales is thanked for X-ray scattering experiments. Jana Falkenhagen is thanked for mass spectrometry. Yannick Wägner is thanked for artificial weathering exposure and IR spectroscopy.

Conflicts of interest

The authors declare no conflict of interest.

Notes and references

1 T. Lee, P. T. Dirlam, J. T. Njardarson, R. S. Glass and J. Pyun, *J. Am. Chem. Soc.*, 2022, **144**, 5–22.
2 2D. Braatz, M. Cherri, M. Tully, M. Dimde, G. Ma, E. Mohammadifar, F. Reisbeck, V. Ahmadi, M. Schirner and R. Haag, *Angew. Chem., Int. Ed.*, 2022, **61**, e20220394.
3 (*a*) M. J. H. Worthington, R. L. Kucera and J. M. Chalker, *Green Chem.*, 2017, **19**, 2748–2761; (*b*) Z. Fan, X. Chen, M. Köhn Serrano, H. Schmalz, S. Rosenfeldt, S. Förster, S. Agarwal and A. Greiner, *Angew. Chem., Int. Ed.*, 2015, **54**, 14539–14544; (*c*) S. Bokern, Z. Fan, C. Mattheis, A. Greiner and S. Agarwal, *Macromolecules*, 2011, **44**, 5036–5042.
4 K. A. Stellmach, M. K. Paul, M. Xu, Y.-L. Su, L. Fu, A. R. Toland, H. Tran, L. Chen, R. Ramprasad and W. R. Gutekunst, *ACS Macro Lett.*, 2022, **11**, 895–901.
5 D. H. Kim, W. Jang, K. Choi, J. S. Choi, J. Pyun, J. Lim, K. Char and S. G. Im, *Sci. Adv.*, 2020, **6**, eabb5320.
6 Y. Wang, M. Li, J. Chen, Y. Tao and X. Wang, *Angew. Chem., Int. Ed.*, 2021, **60**, 22547–22553.
7 P. Yuan, Y. Sun, X. Xu, Y. Luo and M. Hong, *Nat. Chem.*, 2021, **14**, 294–303.
8 Y. Zhu, M. Li, Y. Wang, Y. Tao and X. Wang, *Angew. Chem., Int. Ed.*, 2023, **62**, e2023028.
9 E. A. Prebihalo, A. M. Luke, Y. Reddi, C. J. LaSalle, V. M. Shah, C. J. Cramer and T. M. Reineke, *Chem. Sci.*, 2023, **14**, 5689–5698.
10 H. Li, J. Ollivier, S. M. Guillaume and J.-F. Carpentier, *Angew. Chem., Int. Ed.*, 2022, **61**, e202202386.
11 Y. Wang, M. Li, S. Wang, Y. Tao and X. Wang, *Angew. Chem., Int. Ed.*, 2021, **60**, 10798–10805.
12 J. Yuan, W. Xiong, X. Zhou, Y. Zhang, D. Shi, Z. Li and H. Lu, *J. Am. Chem. Soc.*, 2019, **141**, 4928–4935.
13 C. Hardy, G. Kociok-Köhn and A. Buchard, *Chem. Commun.*, 2022, **58**, 5463–5466.
14 J.-L. Yang, Y. Wang, X.-H. Cao, C.-J. Zhang, Z. Chen and X.-H. Zhang, *Macromol. Rapid Commun.*, 2021, **42**, 2000472.
15 S. Rupf, P. Pröhm and A. J. Plajer, *Chem. Sci.*, 2022, **13**, 6355–6365.
16 R. A. Smith, G. Fu, O. McAteer, M. Xu and W. R. Gutekunst, *J. Am. Chem. Soc.*, 2019, **141**, 1446–1451.
17 T.-J. Yue, L.-Y. Wang and W.-M. Ren, *Polym. Chem.*, 2021, **12**, 6650–6666.
18 N. M. Bingham, Z. Abousalman-Rezvani, K. Collins and P. J. Roth, *Polym. Chem.*, 2022, **13**, 2880–2901.
19 A. S. Narmon, C. A. M. R. van Slagmaat, S. M. A. De Wildeman and M. Dusselier, *ChemSusChem*, 2023, **16**, e202202276.
20 A. J. Plajer and C. K. Williams, *Angew. Chem., Int. Ed.*, 2022, **61**, e202104495.
21 S. Kernbichl and B. Rieger, *Engineering Solutions for CO2 Conversion*, John Wiley & Sons, Ltd, 2021, pp. 385–406.
22 C. A. L. Lidston, S. M. Severson, B. A. Abel and G. W. Coates, *ACS Catal.*, 2022, **12**, 11037–11070.
23 T. M. McGuire and A. Buchard, *Polym. Chem.*, 2021, **12**, 4253–4261.
24 J. Diebler, H. Komber, L. Häußler, A. Lederer and T. Werner, *Macromolecules*, 2016, **49**, 4723–4731.
25 A. J. Plajer, *ChemCatChem*, 2022, **14**, e202200867.
26 D. Silbernagl, H. Sturm and A. J. Plajer, *Polym. Chem.*, 2022, **13**, 3981–3985.
27 P. Deglmann, S. Machleit, C. Gallizioli, S. M. Rupf and A. J. Plajer, *Catal. Sci. Technol.*, 2023, **13**, 2937–2945.
28 T.-J. Yue, M.-C. Zhang, G.-G. Gu, L.-Y. Wang, W.-M. Ren and X.-B. Lu, *Angew. Chem., Int. Ed.*, 2019, **131**, 628–633.
29 X.-L. Chen, B. Wang, D.-P. Song, L. Pan and Y.-S. Li, *Macromolecules*, 2022, **55**, 1153–1164.
30 L.-Y. Wang, G.-G. Gu, T.-J. Yue, W.-M. Ren and X.-B. Lu, *Macromolecules*, 2019, **52**, 2439–2445.
31 L.-Y. Wang, G.-G. Gu, B.-H. Ren, T.-J. Yue, X.-B. Lu and W.-M. Ren, *ACS Catal.*, 2020, **10**, 6635–6644.
32 T.-J. Yue, L.-Y. Wang, W.-M. Ren and X.-B. Lu, *Eur. Polym. J.*, 2023, **190**, 111985.
33 J. Xu, P. Zhang, Y. Yuan and N. Hadjichristidis, *Angew. Chem., Int. Ed.*, 2023, **62**, e2022188.
34 M. Luo, X.-H. Zhang and D. J. Darensbourg, *Macromolecules*, 2015, **48**, 5526–5532.
35 C. Fornacon-Wood, B. R. Manjunatha, M. R. Stühler, C. Gallizioli, C. Müller, P. Pröhm and A. J. Plajer, *Nat. Commun.*, 2023, **14**, 4525.
36 D. J. Darensbourg, *Green Chem.*, 2019, **21**, 2214–2223.
37 X.-L. Li, R. W. Clarke, J.-Y. Jiang, T.-Q. Xu and E. Y.-X. Chen, *Nat. Chem.*, 2023, **15**, 278–285.
38 N. Lucas, C. Bienaime, C. Belloy, M. Queneudec, F. Silvestre and J.-E. Nava-Saucedo, *Chemosphere*, 2008, **73**, 429–442.
39 OECD, *Plastic waste by end-of-life fate and region-projections*, Organisation for Economic Co-operation and Development, Paris, 2022.

